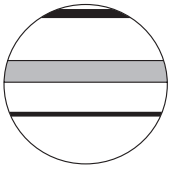

Research Paper

The Holocene
2023, Vol. 33(5) 581–591

DOI: 10.1177/09596836231151835
journals.sagepub.com/home/hol

Radiocarbon sampling efforts for high-precision lake sediment chronologies

Fabian Rey,[1,2,3] Colin J. Courtney Mustaphi,[1] Sönke Szidat,[3,4] Erika Gobet,[2,3] Oliver Heiri[1] and Willy Tinner[2,3]

Abstract

High-resolution chronologies with the best time control are key for comparing palaeoenvironmental studies with independent high-precision historical, archaeological or climatic data. Precise chronologies are also essential for inter-site comparisons of palaeo records at decadal to centennial time scales. We present an updated sediment chronology from Burgäschisee, a small and well-studied lake in the Swiss lowlands. The new age-depth relationship was generated using a large number of new radiocarbon samples of terrestrial plant remains extracted from the Burgäschisee sediments and Bayesian age-depth modelling. The results reveal 2σ uncertainties of only ±19 years for the entire record covering the Early Bronze Age (3800 cal. BP) to the Early Middle Ages (1150 cal. BP). The differences between four age-depth modelling techniques (Bayesian and non-Bayesian) are minor (around 25 years) and remain stable with lower radiocarbon date availability. The maximum age offset between the preliminary previously published and the refined chronology from Burgäschisee is 225 years. Our results demonstrate the importance of a rigorous subsampling strategy that includes a careful selection of the best terrestrial plant material and avoiding radiocarbon calibration plateaus whenever possible. The new chronology from Burgäschisee now allows a more accurate site-to-site comparison with archaeological, historical and other palaeoecological evidence from the region.

Keywords

age-depth modelling, AMS dating, Bacon, clam, OxCal, varved lake sediments

Received 8 August 2022; revised manuscript accepted 21 December 2022

Introduction

Robust chronologies of lake sediments are crucial for interpreting the timing of events and rates of change in palaeoenvironmental reconstructions. For late Quaternary lake sediment sequences, and particularly records covering the Holocene, radiocarbon dating is often the method of choice, with a clear development towards higher resolution dating in the last decades (Trachsel and Telford, 2017). This development resulted in recent chronologies with significantly larger numbers of dated horizons (up to five per 1000 years, e.g. Haas et al., 2020; Kleinmann et al., 2015) compared with earlier studies that typically were based on ca. 10–15 dates for a complete Holocene stratigraphy (e.g. Heiri et al., 2003; Schwörer et al., 2014). Pioneer sedimentary studies with five or more date determinations per 1000 years occur in the 1980s and 1990s (e.g. Ammann and Lotter, 1989; Hajdas et al., 1995), however, such large numbers of radiocarbon dates still remain exceptional. Indeed, recently published sedimentary studies usually include records based on a similar number of radiocarbon ages as earlier studies, resulting in records with intermediate chronological precision (e.g. Duprat-Oualid et al., 2017; Garcés-Pastor et al., 2022; Gassner et al., 2020; Rösch et al., 2021). These chronologies generally have relatively wide 95% (2σ) probabilities of many decades to several hundred calibrated years in some cases, resulting in large chronological uncertainties (e.g. Brugger et al., 2016; Pedrotta et al., 2021; Rey et al., 2022) that affect data comparisons and interpretations. Centennial-scale uncertainties may be sufficient for most records dealing with long-term changes at centennial to millennial time scales (e.g. biological invasion, expansion and decline of species, turnover of species composition). However, thorough site-to-site comparisons at decadal time scales (e.g. short-term land use phases, detailed successional patterns) are only possible with more precise chronologies (e.g. Kleinmann et al., 2015; Rey et al., 2019a). Higher numbers of radiocarbon dates that also include a selection of radiocarbon samples with narrow calibration ranges ($2\sigma < \pm 100$ years) may improve the chronological precision significantly (Rey et al., 2019b, 2020). Refined, Bayesian approaches that are available for radiocarbon dating and age estimation such as OxCal 4.4 (Bronk Ramsey, 1994, 1995) or Bacon 2.5.8 (Blaauw and Christen, 2011) benefit from such a larger number of dated horizons and a higher density of ages along the record (Blaauw and Heegaard, 2012; Blaauw et al., 2018; Trachsel and Telford, 2017). Regarding the choice of suitable material for radiocarbon dating, short-lived terrestrial plant remains (leaves, fruits, seeds, bud scales, fruit scales, needles) should be preferentially selected. Dating of medium- to long-lived plant material (wood), bulk sediments, woody charcoal fragments or aquatic plant remains often results in inaccurate

[1]Geoecology, Department of Environmental Sciences, University of Basel, Switzerland
[2]Institute of Plant Sciences, University of Bern, Switzerland
[3]Oeschger Centre for Climate Change Research, University of Bern, Switzerland
[4]Department of Chemistry, Biochemistry and Pharmaceutical Sciences, University of Bern, Switzerland

Corresponding author:
Fabian Rey, Geoecology, Department of Environmental Sciences, University of Basel, Klingelbergstrasse 27, Basel, Basel-Stadt 4056, Switzerland.
Email: fabian.rey@unibas.ch

radiocarbon dates that are generally too old (Björck and Wohlfahrt, 2001; Ilyashuk et al., 2009; Oswald et al., 2005). Further chronological improvements can be achieved with varve counting (e.g. Lotter, 1999) and a combination of radiocarbon dating with varve based age estimates (e.g. Martin-Puertas et al., 2021; Rey et al., 2019b; Zander et al., 2020; Zolitschka et al., 2015), though varved lake sediments are exceptional archives and rather rare.

In this study, we present a revised, high resolution radiocarbon chronology from Burgäschisee, a small Central European lake, covering the time period from the Early Bronze Age (ca. 3800 cal. BP; cal. BP = calibrated years before present where 'present' equals the 1950th year of the Common Era) to the Early Middle Ages (ca. 1150 cal. BP). The lake is situated in the western Swiss Plateau and its sediments are known to have well-preserved varves (Rey et al., 2017). Pollen analysis of the sediments allowed an assessment of past vegetation changes at the site during the interval of interest. The record has previously been dated using an intermediate (i.e. one radiocarbon date every 1000 years) number of dated horizons across the Holocene, which is here expanded by an additional 56 radiocarbon dates covering the time interval from ca. 3800–1150 cal. BP, leading to an average of 21 radiocarbon dated horizons per 1000 years. We use an approach which is based on radiocarbon wiggle matching and has recently been applied at Burgäschisee and a second Swiss lowland lake, Moossee, for obtaining high-precision chronologies for the Neolithic (ca. 7000–4000 cal BP; Rey et al., 2019b). We then discuss the potential and advantages of such high-resolution lake sediment chronologies in contrast to records with lower chronological resolution, but also how such high-resolution chronologies can provide valuable information for sampling and dating schemes for future studies with fewer resources and radiocarbon dates. We briefly discuss dissimilarities with an earlier chronology from Burgäschisee and the effect of the new chronology on the comparison of the pollen record with other sites in Europe that applied the same (Makri et al., 2020, 2021; Rey et al., 2019a, 2019b, 2020) or similar approaches (e.g. Feeser et al., 2016; Martin-Puertas et al., 2021; Mellström et al., 2013; Zander et al., 2020, 2021) to explore decadal-scale linkages between archaeological, historical and paleoenvironmental events.

Materials and methods

During a first field work expedition at Burgäschisee, Switzerland in fall 2009, three parallel sediment cores (Burg A–C) were retrieved from the deepest part of the lake (water depth: 31 m) with a UWITEC piston corer (core diameter: 6 cm, core length: 300 cm, Rey et al., 2017). In spring 2014, an additional two parallel sediment cores (Burg J, K) were taken at Burgäschisee with a larger UWITEC piston corer (core diameter: 9 cm, core length: 200 cm, Rey et al., 2019a, 2019b). Some weeks later in spring 2014, using the same coring device, three parallel sediment cores (Moos F–G) were retrieved at Moossee, Switzerland (Rey et al., 2019a, 2019b, 2020). At Burgäschisee, a total coring depth of 15 m was reached, resulting in a bottom age of ca. 18,700 cal. BP (Rey et al., 2017). For this study, we focus on the Early Bronze Age to the Early Middle Ages (ca. 3800–1150 cal. BP) during which the sediments at Burgäschisee show continuous and well-preserved varves.

A preliminary study from Burgäschisee was published in 2017 (Rey et al., 2017). The chronology of this study is based on three radiocarbon dates only for the corresponding time interval (ca. 3800–1150 cal. BP, i.e. one radiocarbon date every 1000 years) and the varves were not considered in the age-depth model calculations (Supplemental Table SI, available online). The recently published chronology from Moossee covering the same time window consists of 22 radiocarbon samples (Rey et al., 2020), resulting in an average of ca. eight radiocarbon dates per 1000 years. Here, radiocarbon wiggle matching techniques were applied for the varved sediment parts (Supplemental Table SII, available online). For comparisons in this paper, the chronologies were re-calibrated (Supplemental Tables SI, SII, available online) according to the updated radiocarbon calibration curve (IntCal20, Reimer et al., 2020).

For this study, the sediment of the Burg J and K cores was cut into slices of approximately 10 years (following the varve counts) using the same subsampling procedure as presented in Rey et al. (2019b). This resulted in a total of 295 contiguous samples encompassing the same amount of time (as estimated from the varves) and with a mean volume of 34 cm^3. Samples were collected and washed through a sieve (mesh width: 200 µm) to find suitable plant remains for radiocarbon dating. Only short-lived terrestrial plant material that decomposes rapidly unless preserved in water-saturated sediments (i.e. bud scales, fruits or leaf fragments) was selected. Altogether, 56 samples were measured at LARA, University of Bern (Szidat et al., 2014, Table 1), resulting in an average of 21 radiocarbon dates per 1000 years which increases the dating resolution of the given time interval by almost an order of magnitude compared to the initial study by Rey et al. (2017).

For the new high-resolution Burgäschisee age-depth model (Figure 1a), the V-sequence model of OxCal 4.4 (Bronk Ramsey, 1994, 1995, 2001; Bronk Ramsey et al., 2001) was applied (for OxCal code see Dataset S1). OxCal V-sequence is a Bayesian model that considers a given number of radiocarbon ages (= events), known gaps between events (= varve counts) and additional uncertainties for varve count uncertainties to run the calculations. The model tries to find the best fit directly on the radiocarbon calibration curve (= radiocarbon wiggle matching) based on both radiocarbon dates and the available varve counts.

Three other age-depth modelling approaches were used for comparing the performance of the high-resolution chronology based on OxCal V-sequence (Figures 1 and 2) relative to other methodologies. OxCal P-sequence (Bronk Ramsey, 2008; Bronk Ramsey and Lee, 2013) is a Bayesian age-depth modelling approach that tries to find the best fit of the radiocarbon ages (= events) on the radiocarbon calibration curve based on changes in the sedimentation accumulation rate between events. The P-sequence model allows for fluctuations in the sedimentation accumulation rate between events by adding a parameter *k*. High values of *k* (i.e. 10 or higher) only allow for little to no fluctuations and is tantamount to almost constant sedimentation accumulation rates. Bacon 2.5.8 (Blaauw and Christen, 2011) is another Bayesian model that aims to reconstruct accumulation histories of, for example lake sediment records. The model output is based on a combination of radiocarbon ages and prior assumptions about accumulation rates and their variation over time, but does not take the varve counts into account. Otherwise, the Bacon model looks for the best fit on the radiocarbon curve as well and usually gets more precise with higher numbers of radiocarbon ages used for the model calculations. Clam 2.5.0 (Blaauw, 2010) is a non-Bayesian model based on Monte Carlo sampling with a given number of iterations (e.g. 1000) and interpolation by, for example a smooth-spline through each iteration, creating a weighted mean at a specific sediment depth. This age-depth modelling technique is widely used for records with relatively low numbers of radiocarbon dates and was used for the previously published Burgäschisee chronology (Rey et al., 2017) and for parts of the Moossee chronology (Rey et al., 2020) as well. To investigate the effects of the number of dated horizons on the models, all model runs (OxCal V-sequence, OxCal P-sequence, Bacon and clam) were repeated under reduced radiocarbon date availability (Figures 3 and 4). In this second model run, only radiocarbon ages with 95% (2σ) probabilities $< \pm 100$ cal. years were considered (number of remaining radiocarbon ages: 21) and

Table 1. Radiocarbon dates, calibrated and modelled ages from the new Burgäschisee record (Burg J, K cores). Uncertainties of radiocarbon ages refer to 68% probabilities (1σ) whereas ranges of calibrated and modelled ages represent 95% probabilities (2σ).

Lab. code	Depth (cm)	^{14}C age (BP)[a]	Age (cal. BP)[b]	Modelled age (cal. BP)[c]	Material
BE-7528.1.1	223.3–221.5	1215 ± 20	1065–1240	1115–1158	*Betula* fruit, *Populus tremula* floral bract, *Fagus sylvatica* bud scales, bud scale indet
BE-7527.1.1	223.5	1210 ± 20	1065–1240	1130–1165	*Fagus sylvatica* leaf fragments
BE-7526.1.1	225.2–224.2	1175 ± 30	975–1175	1145–1170	*Fagus sylvatica* bud scales
BE-7525.1.1	226.7–225.9	1115 ± 30	935–1175	1165–1180	*Betula* fruit, *Betula* fruit scale, *Fagus sylvatica* bud scale
BE-7524.1.1	234.7–233.7	1260 ± 30	1075–1280	1240–1265	*Fagus sylvatica* bud scales
BE-7523.1.1	235.3	1335 ± 20	1180–1300	1260–1285	*Fagus sylvatica* leaf fragments
BE-7522.1.1	238.7–237.9	1340 ± 30	1175–1305	1285–1310	*Fagus sylvatica* bud scales
BE-7521.1.1	242.0–241.3	1455 ± 20	1305–1370	1320–1345	*Fagus sylvatica* bud scales
BE-7520.1.1	243.6–242.0	1435 ± 30	1295–1370	1330–1360	*Fagus sylvatica* bud scales
BE-7519.1.1	249.0–247.4	1625 ± 20	1415–1540	1410–1435	*Fagus sylvatica* bud scales
BE-7518.1.1	257.6–256.0	1575 ± 35	1385–1530	1495–1525	*Fagus sylvatica* bud scales
BE-7517.1.1	258.2–257.6	1580 ± 30	1395–1530	1510–1540	*Fagus sylvatica* bud scales
BE-7516.1.1	259.5–258.2	1665 ± 30	1415–1690	1525–1565	*Betula* fruits, *Populus tremula* floral bract, *Fagus sylvatica* bud scales
BE-7515.1.1	262.6–260.3	1700 ± 30	1530–1695	1555–1605	*Betula* fruits, *Fagus sylvatica* bud scales, bud scale indet
BE-7514.1.1	270.1–267.6	1760 ± 35	1550–1720	1650–1705	*Betula* fruits, *Fagus sylvatica* bud scale, *Quercus* bud scale
BE-7513.1.1	286.3–283.7	1920 ± 30	1740–1925	1810–1860	*Betula* fruits, *Fagus sylvatica* bud scales, *Quercus* bud scale
BE-7512.1.1	287.7–286.3	1930 ± 20	1745–1925	1835–1875	*Betula* fruits, *Fagus sylvatica* bud scales
BE-7511.1.1	290.4–287.7	1905 ± 30	1730–1920	1850–1890	*Betula* fruits, *Fagus sylvatica* bud scales, *Quercus* bud scale
BE-7510.1.1	294.6–292.7	1925 ± 20	1745–1920	1900–1935	*Betula* fruit, *Fagus sylvatica* bud scales
BE-13415.1.1	306.3–305.6	2140 ± 15	2010–2295	2085–2125	*Fagus sylvatica* leaf fragments
BE-13414.1.1	313.3–312.6	2245 ± 35	2150–2340	2180–2215	*Fagus sylvatica* bud scale
BE-13413.1.1	314.7–314.0	2220 ± 15	2150–2315	2200–2235	*Fagus sylvatica* bud scales
BE-13412.1.1	318.3–317.6	2165 ± 15	2100–2300	2260–2290	*Betula* fruit, *Fagus sylvatica* bud scales
BE-13411.1.1	324.0–323.5	2430 ± 25	2355–2695	2355–2385	*Betula* fruit, *Fagus sylvatica* bud scales
BE-13410.1.1	325.3–324.6	2430 ± 15	2360–2680	2375–2405	*Fagus sylvatica* bud scales, *Fagus sylvatica* leaf fragments, bud scale indet
BE-14277.1.1	335.8–335.2	2435 ± 20	2360–2695	2420–2450	*Betula* fruit scale, *Betula* leaf fragments
BE-14276.1.1	351.6–350.9	2450 ± 30	2360–2700	2655–2685	*Fagus sylvatica* bud scales
BE-14275.1.1	352.1–351.6	2460 ± 30	2365–2705	2665–2695	*Fagus sylvatica* bud scale, leaf fragments indet
BE-14274.1.1	352.7–352.1	2460 ± 20	2370–2705	2675–2705	*Fagus sylvatica* bud scales leaf fragments indet
BE-14273.1.1	360.7–360.1	2760 ± 30	2775–2935	2810–2840	*Abies alba* seed wing, *Fagus sylvatica* bud scales
BE-14272.1.1	361.3–360.7	2735 ± 20	2775–2870	2820–2855	*Betula* fruits, *Betula* fruits scale, *Fagus sylvatica* bud scales
BE-14271.1.1	361.9–361.3	2720 ± 30	2760–2865	2835–2870	*Betula* fruit, *Fagus sylvatica* bud scales
BE-14270.1.1	368.3–367.8	2790 ± 30	2785–2960	2935–2970	*Betula* fruits scale, *Fagus sylvatica* bud scale
BE-14269.1.1	368.9–368.3	2845 ± 20	2870–3055	2950–2990	*Fagus sylvatica* bud scales
BE-14268.1.1	372.6–371.9	2915 ± 30	2965–3160	3015–3055	*Betula* fruits, *Fagus sylvatica* bud scales
BE-14267.1.1	373.2–372.6	2940 ± 20	3005–3165	3030–3070	*Betula* fruit, *Betula* fruit scale, *Fagus sylvatica* bud scales
BE-14266.1.1	373.9–373.2	2945 ± 20	3005–3170	3050–3085	*Fagus sylvatica* bud scales, *Fagus sylvatica* leaf fragments
BE-14265.1.1	374.4–373.9	2940 ± 20	3005–3165	3065–3100	*Betula* bud scale, *Betula* fruit, *Betula* leaf fragments, *Fagus sylvatica* bud scales, bud scale indet
BE-14264.1.1	379.4–378.7	2960 ± 30	3005–3215	3125–3160	*Fagus sylvatica* bud scales, bud scale indet
BE-14263.1.1	381.9–381.4	3025 ± 20	3160–3335	3155–3190	*Betula* fruit, *Fagus sylvatica* bud scales
BE-14262.1.1	389.5–388.9	3055 ± 30	3175–3355	3220–3255	*Alnus* bud scale, *Alnus* fruit
BE-14261.1.1	391.2–390.7	3050 ± 15	3180–3345	3240–3270	*Betula* fruit scale, *Fagus sylvatica* bud scales, bud scale indet
BE-14260.1.1	395.5–394.8	3050 ± 25	3175–3350	3290–3320	*Betula* fruit, *Fagus sylvatica* bud scales
BE-14259.1.1	396.1–395.5	3035 ± 25	3165–3345	3305–3335	*Betula* fruit, *Fagus sylvatica* bud scales
BE-14258.1.1	397.2–396.6	3120 ± 25	3245–3440	3330–3355	*Fagus sylvatica* bud scales
BE-14257.1.1	406.3–405.7	3290 ± 15	3455–3560	3450–3475	*Abies alba* bud scale, *Betula* fruit, *Fagus sylvatica* leaf fragment
BE-14256.1.1	411.8–411.1	3305 ± 25	3460–3570	3510–3545	*Fagus sylvatica* leaf fragment
BE-14255.1.1	419.4–418.9	3345 ± 25	3485–3680	3595–3635	*Abies alba* needle, *Betula* fruit, *Betula* leaf fragment, *Fagus sylvatica* bud scale
BE-14254.1.1	420.6–420.0	3415 ± 25	3575–3815	3610–3660	*Alnus* bud scale, *Betula* fruits, *Fagus sylvatica* bud scale, bud scale indet
BE-14253.1.1	421.9–421.2	3355 ± 25	3490–3685	3625–3680	*Betula* fruits, *Betula* fruit scales
BE-14252.1.1	422.5–421.9	3420 ± 25	3575–3820	3635–3695	*Abies alba* bud scale, *Betula* bud scale, *Betula* fruits, *Betula* fruit scales, *Fagus sylvatica* bud scale
BE-14251.1.1	423.7–423.1	3470 ± 25	3645–3830	3650–3715	*Abies alba* needle, *Betula* fruit, *Quercus* bud scales
BE-14250.1.1	425.5–424.9	3470 ± 25	3645–3830	3680–3740	*Abies alba* needle, *Betula* fruits
BE-14249.1.1	428.7–428.0	3530 ± 25	3700–3895	3725–3790	*Fagus sylvatica* bud scales
BE-14248.1.1	429.3–428.7	3545 ± 30	3720–3960	3730–3800	*Abies alba* needle, *Betula* fruit scales
BE-5405.1.1	432.2–431.6	3530 ± 20	3720–3885	3765–3840	*Fagus sylvatica* bud scale, *Fagus sylvatica* leaf fragments

[a]Stuiver and Polach (1977).
[b]IntCal20: Stuiver and Reimer (1993), Reimer et al. (2020).
[c]OxCal V-sequence: Bronk Ramsey (1994, 1995, 2001), Bronk Ramsey et al. (2001).

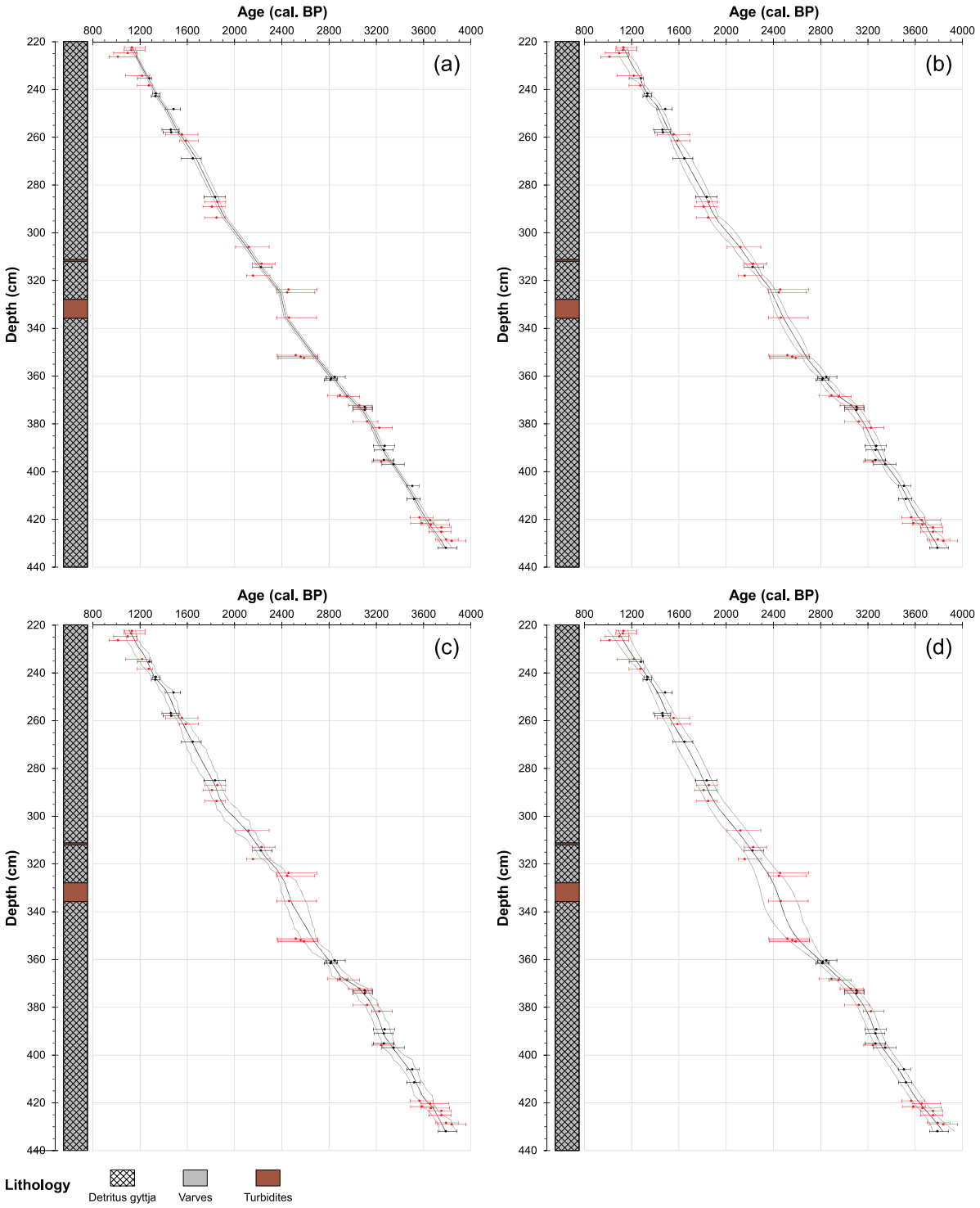

Figure 1. Compilation of different age-depth models and lithology of the new Burgäschisee record (Burg J, K cores). Black and red dots show the calibrated ages with 95% (2σ) probabilities (IntCal20; Reimer et al., 2020). The ages coloured in black have 95% confidence ranges $< \pm 100$ years (see Figures 3 and 4). The black lines are the modelled chronologies and the grey lines represent the 95% (2σ) probabilities of the models. (a) Main model: OxCal V-sequence (Bronk Ramsey, 1994, 1995, 2001; Bronk Ramsey et al., 2001). (b) Comparison model: OxCal P-sequence (parameter $k = 1$; Bronk Ramsey, 1994, 1995, 2001, 2008; Bronk Ramsey and Lee, 2013). (c) Comparison model: Bacon (priors: mean accumulation rate = 20 years/cm, accumulation shape = 1.5; Blaauw and Christen, 2011). (d) Comparison model: clam (smooth spline at smoothing level = 0.65; Blaauw, 2010).

compared to the previously calculated, high-resolution OxCal V-sequence age-depth model from the first run.

For the comparison of the old Burgäschisee chronology (Burg A–C cores, Rey et al., 2017) with the new, updated chronology (Burg J, K cores, this study), the depths of the radiocarbon dates from the old sediment cores were transferred to the new sediment cores (Figure 2, Supplemental Table SIII, available online) based on detailed lithostratigraphic markers (e.g. distinct varve sequences). The same procedure was applied to the depths of the published pollen samples (Figure 5, Supplemental Table SIII, available online; Rey et al., 2017).

Results

The new OxCal V-sequence for the Burgäschisee sediment record has a model agreement index of 60.3 and an overall agreement

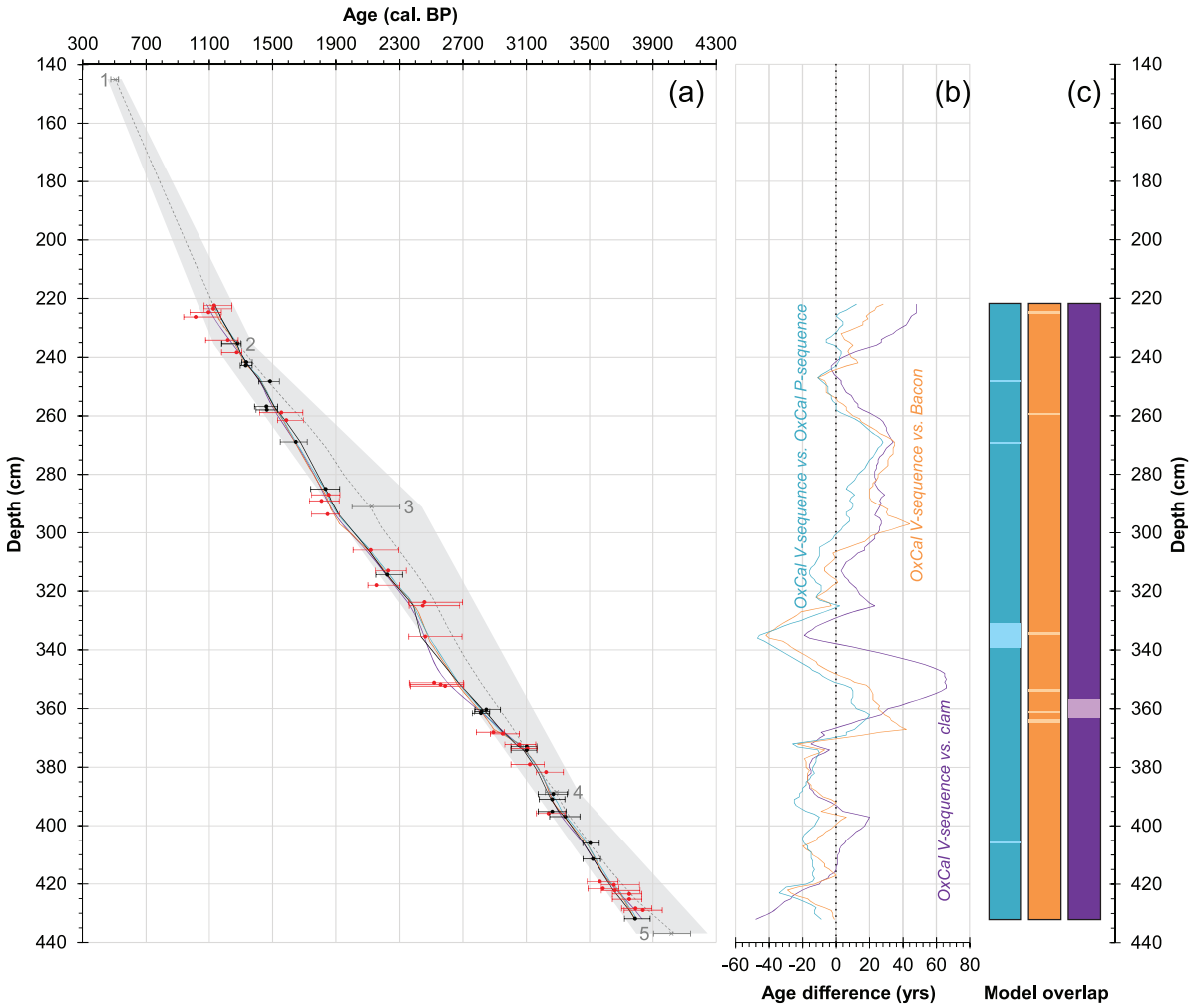

Figure 2. (a) Comparison of different age-depth modelling approaches for Burgäschisee. Grey crosses (1–5) indicate the calibrated ages with 95 % (2σ) probabilities (IntCal20; Reimer et al., 2020) of the old Burg A–C cores. Burg A–C depths were correlated to the Burg J, K cores based on lithological features of the sediment (Table SIII). The grey dashed line represents the chronology of the old Burg A–C cores including the model envelope based on GAM modelling (light grey shaded area; Rey et al., 2017). Black and red dots show the calibrated ages with 95 % (2σ) probabilities (IntCal20; Reimer et al., 2020) of the new Burg J, K cores. The ages coloured in black have 95 % confidence ranges < ±100 years (see Figures 3 and 4). Black line = OxCal V-sequence (main model; Bronk Ramsey, 1994, 1995, 2001; Bronk Ramsey et al., 2001), turquoise line = OxCal P-sequence (parameter k = 1; Bronk Ramsey, 1994, 1995, 2001, 2008; Bronk Ramsey and Lee, 2013), orange line = Bacon (priors: mean accumulation rate = 20 years/cm, accumulation shape = 1.5; Blaauw and Christen, 2011), purple line = clam (smooth spline at smoothing level = 0.65; Blaauw, 2010). Only the mean model runs are shown. For 95 % (2σ) probabilities of the age-depth models see Figure 1. (b) Age differences between the mean model runs of OxCal V-sequence versus OxCal P-sequence (turquoise line), OxCal V-sequence versus Bacon (orange line) and OxCal V-sequence versus clam (purple line). (c) Model overlaps between the model envelopes (Figure 1) of OxCal V-sequence and OxCal P-sequence (turquoise bar), OxCal V-sequence and Bacon (orange bar) and OxCal V-sequence and clam (purple bar). Dark colouring = full model overlap, light colouring = partial model overlap.

index of 61.5 (acceptable minimum model index: 60.0). All 56 radiocarbon dates were included in the model calculations (Figure 1a, Table 1). Thirty-five radiocarbon dates have 95% (2σ) probabilities > ± 100 cal. years (red dots in Figures 1 and 2) and the remaining 21 radiocarbon dates have 95% (2σ) probabilities < ± 100 cal. years (black dots in Figures 1–4). The final age-depth model (Figure 1a) has very narrow 95% (2σ) age probabilities. The mean modelled uncertainty is ±19 years (2σ), with maximum precisions of ±8 years (2σ) reached around 1170 cal. BP and minimum precisions of ±36 years (2σ) in the very bottom part of the examined interval (at around 3800 cal. BP).

The sedimentation accumulation rates are not constant but more or less stable at around 12.6 years/cm. One prominent turbidite layer (thickness: 8 cm) could be detected visually and was defined as single geologically instantaneous event since the three radiocarbon dates just below and above the event layer have all very similar calibrated ages. This would not be the case if the average sedimentation accumulation rate would be applied to the turbidite layer as well, resulting in a hypothetical age range of ca. 100 years for the 8 cm of sediment.

The comparison between the main age-depth model (OxCal V-sequence, Figure 1a) and the OxCal P-sequence, Bacon as well as clam model outputs reveals rather surprisingly small age differences among the different age depth modelling methods (Figure 2). The age differences are most of the time below or at 25 years (Figure 2b). The maximum age difference between OxCal V-sequence (Bayesian) and clam (non-Bayesian) is <70 years whereas the age offset between the three Bayesian models (OxCal V-sequence, OxCal P-sequence and Bacon) is noticeably smaller (<45 years). The maximum age difference between the OxCal V-sequence and the clam model outputs falls into a prominent plateau of the radiocarbon calibration curve between ca. 2750 and 2350 cal. BP (Reimer et al., 2020). Three neighbouring radiocarbon samples (BE-14274.1.1, BE-14275.1.1, BE-14276.1.1, Table 1) are all located in this radiocarbon plateau as indicated by wide calibration ranges (2σ). These three radiocarbon dates are mainly causing the maximum age

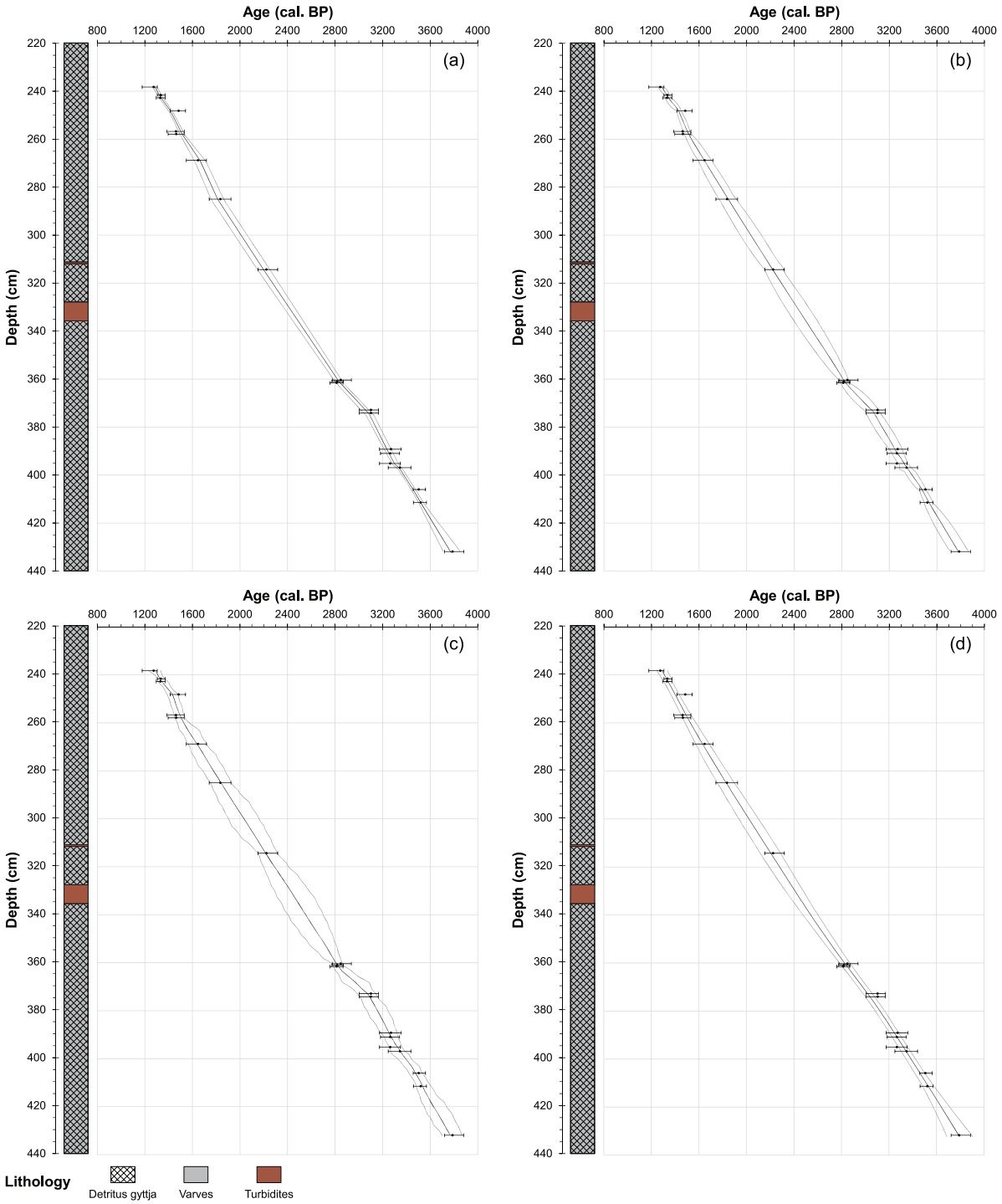

Figure 3. Compilation of different age-depth models and lithology of Burgäschisee under reduced radiocarbon dates availability (see Figures 1 and 2 for full record). Black dots show the calibrated ages with 95% (2σ) probabilities $< \pm 100$ years (IntCal20; Reimer et al., 2020) of the new Burg J, K cores. The black lines are the modelled chronologies and the grey lines represent the 95% (2σ) probabilities of the models. Only ages with 95% confidence ranges $< \pm 100$ years were included in the model runs. (a) OxCal Vsequence (Bronk Ramsey, 1994, 1995, 2001; Bronk Ramsey et al., 2001). (b) OxCal P-sequence (parameter $k = 1$; Bronk Ramsey, 1994, 1995, 2001, 2008; Bronk Ramsey and Lee, 2013). (c) Bacon (priors: mean accumulation rate = 20 years/cm, accumulation shape = 1.5; Blaauw and Christen, 2011). (d) Clam (smooth spline at smoothing level = 0.65; Blaauw, 2010).

difference that results from the strong weighting of the median cal. ages in the clam model calculations (Blaauw, 2010). Most of the time, there is a full model overlap between the model envelopes of OxCal V-sequence and the other three age-depth modelling approaches (Figure 2c) which means that the very narrow (or less uncertain) model envelope of the OxCal V-sequence model is generally completely incorporated in the wider (or more uncertain) model envelopes of the other three age-depth models.

One radiocarbon date from the old chronology from Burgäschisee, which was calculated with the programme clam using a smooth-spline curve (smoothing level: 0.23, Rey et al., 2017), strongly influences the age-depth model output. The comparison between the new chronology (OxCal V-sequence) and the original published chronology (clam) reveals a maximum age difference of 225 years among the two age-depth modelling approaches (Supplemental Table SIII, available online). However, the updated chronology mostly lies within the modelled uncertainty envelope of the old chronology (light grey area in Figure 2), which was calculated using a generalised mixed-effect regression (GAM, Heegaard et al., 2005). The GAM model considers both effects of

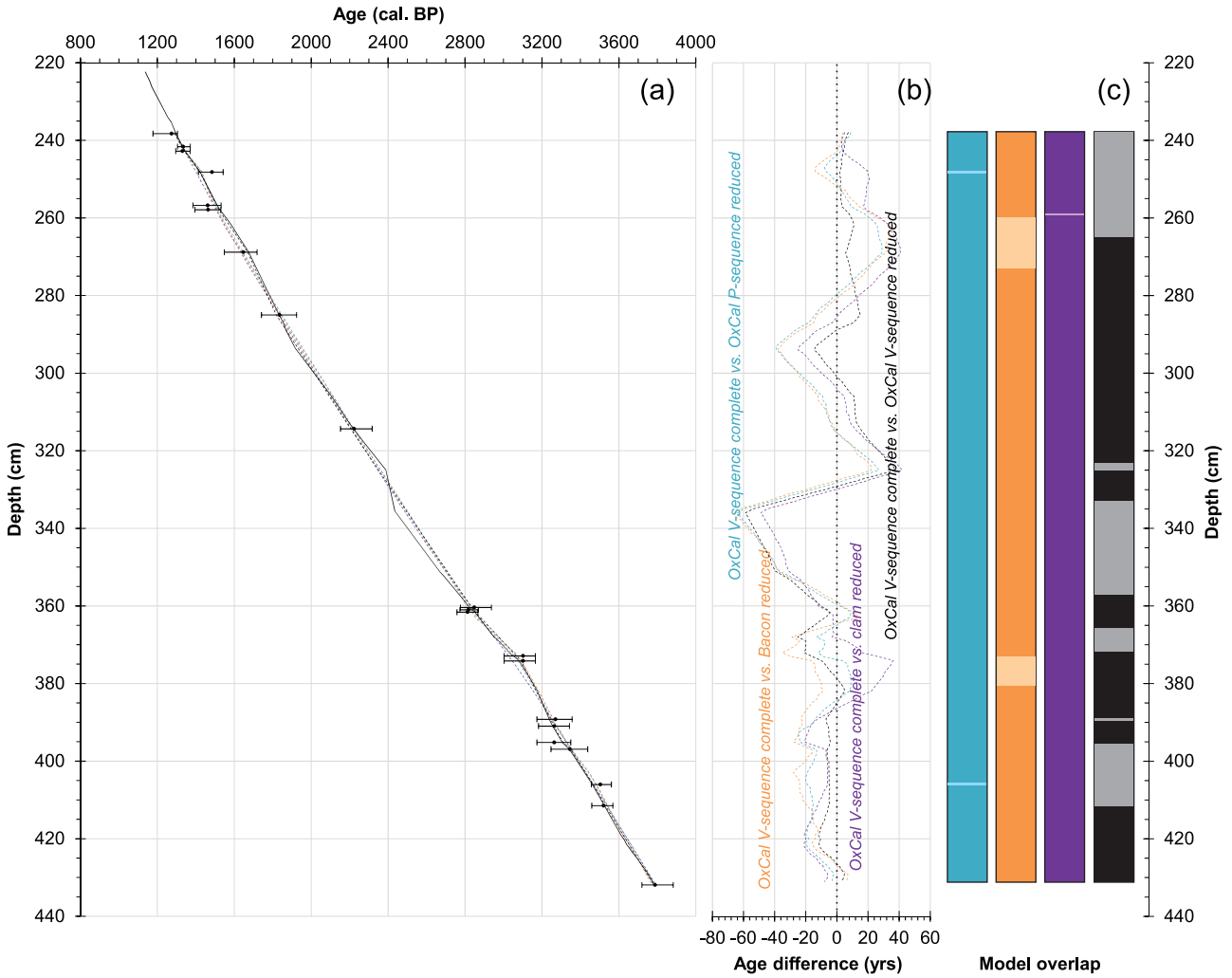

Figure 4. (a) Comparison of different age-depth modelling approaches for Burgäschisee under reduced radiocarbon dates availability (see Figures 1 and 2 for full record). Black dots show the calibrated ages with 95% (2σ) probabilities < ±100 years (IntCal20; Reimer et al., 2020) of the new Burg J, K cores. Black lines (solid and dashed) = OxCal V-sequence (Bronk Ramsey, 1994 , 1995, 2001; Bronk Ramsey et al., 2001), turquoise dashed line = OxCal P-sequence (parameter *k* = 1; Bronk Ramsey, 1994, 1995, 2001, 2008; Bronk Ramsey and Lee, 2013), purple dashed line = clam (smooth spline at smoothing level = 0.65; Blaauw, 2010), orange dashed line = Bacon (priors: mean accumulation rate = 20 years/cm, accumulation shape = 1.5; Blaauw and Christen, 2011). Only the mean model runs are shown. For 95% (2σ) probabilities of the age-depth models see Figure 3. Four model runs (dashed lines) only include ages with 95% confidence ranges < ±100 years. The solid black line represents the OxCal V-sequence model run from Figure 2 that includes all radiocarbon ages (main model). (b) Age differences between the mean model runs of OxCal Vsequence (complete data set) versus OxCal P-sequence (reduced data set; turquoise dashed line), OxCal Vsequence (complete data set) versus Bacon (reduced data set; orange dashed line), OxCal V-sequence (complete data set) versus clam (reduced data set; purple dashed line) and OxCal V-sequence (complete data set) versus OxCal V-sequence (reduced data set; black dashed line). Only ages with 95% confidence ranges < ±100 years are included. (c) Model overlaps between the model envelopes (Figure 3) of OxCal Vsequence (complete data set) and OxCal P-sequence (reduced data set; turquoise bar), OxCal V-sequence (complete data set) and Bacon (reduced data set; orange bar), OxCal V-sequence (complete data set) and clam (reduced data set; purple bar) and OxCal V-sequence (complete data set) and OxCal V-sequence (reduced data set; black bar). Dark colouring = full model overlap, light colouring = partial model overlap.

sample depth and age uncertainties. The uncertainty derived from subsampling prior to radiocarbon dating of the preliminary study (Rey et al., 2017) is already substantial (i.e. 3 cm of sample thickness for samples sieved for radiocarbon dating corresponding to ca. 40 years of subsampling uncertainty, whereas for the new chronology sample depth intervals ranged from 0.4 to 1.0 cm depending on the varve counts). Due to a plateau in the radiocarbon calibration curve, the uncertainty further increases after age calibration and age-depth modelling and creates large model uncertainties of up to ±300 years at around 290 cm (ca. 1900 cal BP, Figure 2).

The model runs that only include 21 radiocarbon dates with calibration ranges <100 years (2σ) again show very similar results (Figures 3 and 4). The age differences between the age-depth models are mostly below 25 years with maximum age differences of <50 years (OxCal V-sequence complete versus clam reduced), <60 years (OxCal V-sequence complete versus OxCal V-sequence reduced) and <75 years respectively (OxCal V-sequence complete versus OxCal P-sequence reduced and OxCal V-sequence complete versus Bacon reduced). The model overlaps between the OxCal V-sequence model (including all radiocarbon ages) and the model runs under reduced radiocarbon dates availability remain high (Figure 4c). This result demonstrates the importance of the positioning of each radiocarbon date on the calibration curve (best outside radiocarbon plateaus). Thus, it may be beneficial to split the samples in two (or more) batches prior to the radiocarbon measurements to be able to isolate and avoid potential radiocarbon plateaus after receiving the results of the first batch. High numbers of radiocarbon dates seem to improve the model output of Bayesian age-depth models (OxCal

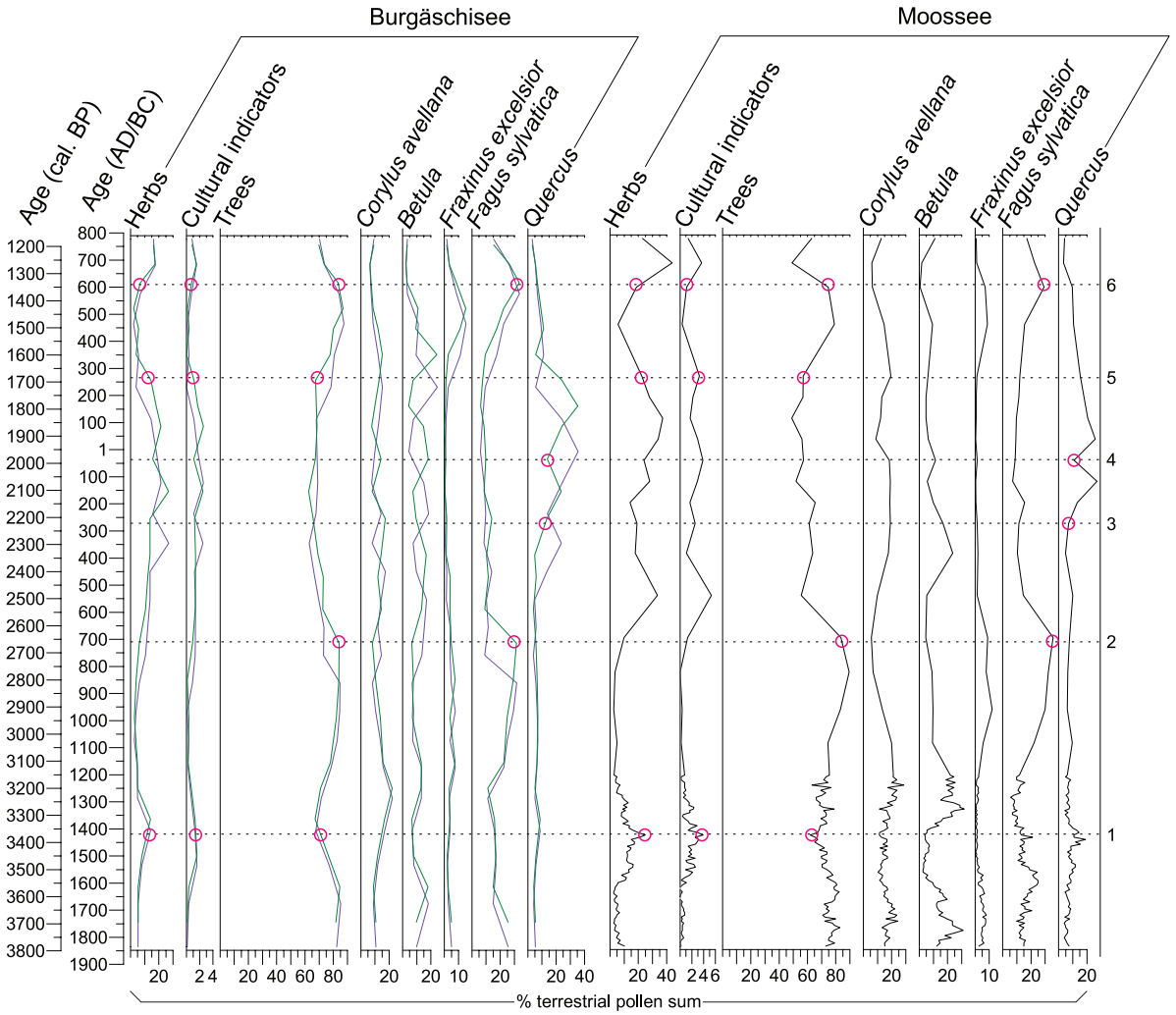

Figure 5. Comparison of the pollen percentages from selected pollen types from the two independently dated lake sediment records of Burgäschisee and Moossee. Purple lines = pollen data from the Burgäschisee record plotted on the old time scale (Rey et al., 2017), green lines = pollen data from the Burgäschisee record based on the new time scale from the main model (Figure 1a), black line = pollen data from the Moossee record (Rey et al., 2020) updated to IntCal20 (Reimer et al., 2020). Dashed lines (1–6) indicate contemporaneous events (highlighted by magenta circles). 1 = Mid Bronze Age land use phase, 2 = onset of Iron Age land use phase, 3 = first anthropogenic favouring of *Quercus*, 4 = *Quercus* minimum, 5 = onset of successional reforestation in the Late Antiquity, 6 = onset of Early Middle Ages land use phase. Cultural indicators = sum of the pollen percentages of Cerealia-type and *Plantago lanceolata*.

P-sequence, Bacon) whereas radiocarbon dates with narrow calibration ranges ($2\sigma < \pm 100$ years) are beneficial for both Bayesian and non-Bayesian age-depth modelling approaches.

Discussion

When all available radiocarbon dates are included, the age-depth model output for Burgäschisee derived from OxCal V-sequence is very much in line with the three other age-depth modelling approaches (OxCal P-sequence, Bacon, clam) which are, together with other age-depth model techniques (e.g. linear interpolation, GAM), all commonly used in palaeoenvironmental studies (e.g. Haas et al., 2020; Kołaczek et al., 2021; Rey et al., 2013; Schwörer et al., 2015). However, OxCal V-sequence provides by far the smallest age uncertainty intervals (Figure 1), because only in this model varve counts are considered. The age differences between the models are generally smaller than 25 years even when applying a lower number of radiocarbon dates with narrow calibration ranges ($2\sigma < 100$ years). This result strikingly demonstrates, at least in the case of Burgäschisee, that having several high-resolution calibrated dates (with narrow age probability intervals) is probably as important as having the highest possible number of radiocarbon dates for the age-depth model calculations. Hence, for studies with limited budgets it may be worthwhile to do a first selection and dating effort with the best material possibly followed by additional sample submissions once initial results are available. This requires a rigorous subsampling strategy which will possibly increase the work load (sieving, identification and selection of suitable plant remains) and if multiple submissions are necessary also the time needed for establishing the final chronology of a record. However, with this procedure, it is still possible to react after receiving the results of the first sample selection and, if needed, send a second batch of samples for chronological improvements that strictly avoids radiocarbon plateaus. In this case, namely with a high number of radiocarbon dates available (in our case eight per 1000 years), non-Bayesian age-depth modelling (clam, GAM) appear to provide reasonable results as well. However, our results show that the clam model can have difficulties in overcoming plateaus in the radiocarbon calibration curve due to wide 95% (2σ) probabilities (generally $> \pm 100$ years), resulting in mean modelled ages that are sometimes considerably different from the most probable calibrated ages of individual samples. Therefore, with more radiocarbon dates available, as is the case in our Burgäschisee chronostratigraphy at maximum resolution, a Bayesian approach (OxCal, Bacon) should be preferred since the age-depth relationship will lead to both more precise and more accurate results (Blaauw and Heegaard, 2012; Blaauw et al., 2018; Trachsel and Telford, 2017).

Further chronological improvements can be achieved by applying a continuous subsampling strategy (Rey et al., 2019b). Narrow (⩽1 cm thick sediment slices) and continuous sampling will reduce the uncertainty derived from subsampling. For instance, in parts of a sediment core with very low sedimentation, a 2 cm-thick sediment slice may already incorporate several hundred years of uncertainty (e.g. Rey et al., 2022), which may even result in a significant bias. In this case and to minimise the subsampling uncertainty and its possible bias, it is worthwhile to increase the sample resolution even if this will almost certainly lead to additional lab work. Equally important as the subsampling is the selection of the best-suited material prior to the radiocarbon measurements. Well-preserved and short-lived terrestrial plant remains (e.g. bud scales, fruits, leaves, needles) proved to give the most reliable results (Goslar et al., 2005; Ilyashuk et al., 2009; Oswald et al., 2005) and should whenever possible be prioritised. In contrast, dating of bulk sediments, long-lived terrestrial plant remains (wood), macroscopic charcoal particles or aquatic plant remains should be avoided as they may give erroneous results which are often too old due to numerous reasons such as hard-water effects, inbuilt ages and reworking of older material (Björck and Wohlfahrt, 2001; Finsinger et al., 2019; Gavin, 2001; Marty and Myrbo, 2014).

The comparison between the new high-precision chronology from Burgäschisee with the old one (Rey et al., 2017) not only reveals age differences between the modelled ages of the radiocarbon samples but also among the pollen samples (Table SIII). The age difference becomes visually evident when the pollen percentages of selected taxa are plotted on the same age scale (Figure 5). Only the trends of the pollen results based on the new chronology (green curves in Figure 5) are in line with the results from the previously published Moossee record (Rey et al., 2020), which was, in itself, based on a large number of dated horizons (eight samples per 1000 years). Rather short-term vegetation changes such as the onset of the Iron Age land use phase at ca. 2650 cal. BP (decrease of tree percentages), the successional trends of *Quercus* between ca. 2200 and 1650 cal. BP and the reforestation after 1700 cal. BP (increase of tree percentages) seemed to occur non-simultaneously around the two lakes on the basis of the old Burgäschisee age-depth model. However, based on the updated chronology, consisting of 21 dated horizons per 1000 years at Burgäschisee compared with eight at Moossee, those changes become synchronous between the two sites which underlines the importance of the chronological framework of palaeoenvironmental records. Although the original Burgäschisee chronology is consistent with the new chronology if the original uncertainty estimates are taken into account (Figure 2), the significantly increased number of radiocarbon dates at Burgäschisee revealed that decadal scale changes in pollen assemblages (and therefore also vegetation) at the two lakes were synchronous rather than asynchronous, as could have been naively assumed based on the original, low resolution radiocarbon stratigraphy from Burgäschisee. Interestingly, the contemporaneous vegetation trends are evident even when applying a rather low temporal and discontinuous resolution of the pollen samples (i.e. one sample every ca. 100 years). Hence, it may be crucial to invest more time in compiling and/ or improving chronologies first rather than investing a major part of the work load in increasing the number of pollen samples, particularly if the interest is focused on comparing decadal scale variations in record with independently dated reconstructions, as is the case in our comparison of vegetation change at Burgäschisee with Moossee. Similar results were obtained for the Neolithic period, with high-precision dating permitting the identification of several synchronous land use phases at Burgäschisee, Moossee and other central and southern European sites (Rey et al., 2019a).

Since paleoenvironmental studies in Europe have a long tradition, the results from numerous sites are available and site-to-site comparisons (e.g. Dietre et al., 2017; Feeser et al., 2016; Gobet et al., 2003), regional compilations (e.g. Kleinmann et al., 2015; Rösch et al., 2014, 2021; Tinner and Theurillat, 2003) and even supra-regional syntheses (Bolland et al., 2020; Rey et al., 2019a, 2020; Tinner et al., 2003, 2005; Vescovi et al., 2007) are very common. The chronological precision of those records is most of the time at centennial-time scales with some exceptions (e.g. Kleinmann et al., 2015; Zander et al., 2021). This means that decadal time-scale research questions should not be addressed (Blaauw and Heegaard, 2012; Rey et al., 2019b). For instance, for thorough inter-site comparisons of land use phases and short-term successional trends (synchronous vs diachronous vegetation patterns in space) higher chronological precisions are needed. Unfortunately, age-depth relationships with precisions at decadal-scale remain very rare (e.g. Kleinmann et al., 2015; Makri et al., 2020, 2021; Martin-Puertas et al., 2021; Mellström et al., 2013; Rey et al., 2019a, 2019b, 2020; Zander et al., 2020, 2021) and quite often the full chronological information is not given since many studies do not show summary tables including the modelled probability ranges and because of that the reliability of the chronologies cannot be thoroughly checked (Lacourse and Gajewski, 2020).

Conclusions

Pioneer studies from the 1980s suggested that establishing excellent sedimentary chronologies requires a very high number of radiocarbon dates on terrestrial plant macrofossils (e.g. Ammann and Lotter, 1989). Since then only a few densely dated sedimentary studies have been achieved, while studies with an intermediate number of dates remained a standard. Our study reveals that the chronology of radiocarbon-dated lake sediment records of Mid- to Late-Holocene age can be significantly improved if the number of dated horizons is increased to similar levels as at Burgäschisee and Moossee, but also if care is taken to submit appropriate material and avoid radiocarbon plateaus. If available, varve counts can decisively reduce age uncertainties (Figure 1, Table 1). Conspicuous and systematic chronological differences up to >200 years between the previously published Burgäschisee chronology with an intermediate number of dates (ca. one date per 1000 years) and our new chronology (21 dates per 1000 years, Figure 2) show that increasing the number of radiocarbon samples beyond one per 1000 years is crucial to gain reliable chronologies at decadal-to centennial-scales. The observation that dating the Burgäschisee record with a high number of dates (ca. eight per 1000 years) resulted in a very similar chronology as when the full, very high number of radiocarbon dates were included (ca. 21 per 1000 years), provided that radiocarbon plateaus were avoided, implies that a critical reflection about the strategies underlying the radiocarbon dating of lake sediment records is needed, particularly concerning comparisons of pollen records. This implies that more resources, both in respect to invested time but also finances, should probably be invested in conducting accurate sedimentary chronologies, as these influence the quality and interpretation of the following sedimentological and palaeoecological analyses, particularly if these are done at very high, decadal-scale resolution. A well-thought-out selection of material prior to the radiocarbon measurement should be considered, especially if finances are limiting in a research project. Short-lived terrestrial plant material (e.g. bud scales, fruits, seeds, leaves, needles) will generally result in more precise radiocarbon dates than dating of bulk sediments, charcoal particles, aquatic plants or long-lived plant material (e.g. wood). Strategies that may help to avoid radiocarbon plateaus and result in calibrated ages with relatively small uncertainty ranges (in our study represented by the radiocarbon ages with an error <100 years) include the submission of several batches of samples, with the initial submission providing a first chronological framework for a record and a second (and possibly further) submission(s) targeting depths

which, based on the initial data, are unlikely to represent radiocarbon plateaus. However, this almost certainly requires additional lab work (continuous subsampling, sieving) and basic knowledge of plant identification. Our comparison of the Burgäschisee and Moossee pollen records reveal that profound site-to-site comparisons at decadal time scales should only be attempted with precise chronologies, as apparent agreements but also mismatches in environmental signals between sites with high multidecadal- to centennial-scale uncertainties may be simply the consequence of age uncertainties rather than actual synchroneities or offsets of signals. Our new, updated chronology from Burgäschisee is now very much in-line with the previously published Moossee study, with uncertainty estimates for the chronologies suggesting that the agreements between the pollen records from these sites is truly due to similar and synchronous vegetation developments at the two sites. These narrow age uncertainty estimates and the synchronous vegetation change at the two sites also provide confidence for comparisons with other palaeoenvironmental records outside the study region and/or independent high-precision archaeological, historical and climate proxy data with low age uncertainty estimates (e.g. tree rings). To conclude, we highly recommend aiming for robust lake sediment chronologies first before increasing the temporal resolution of environmental reconstructions (e.g. continuous, high resolution pollen analysis).

Acknowledgements

We thank Petra Beffa, Sandra O. Brugger, Daniele Colombaroli, Claire Rambeau, Julia Rhiner, Stéphanie Samartin, Christoph Schwörer, Willi Tanner and Lena Thöle for their help during the fieldwork, Edith Vogel for processing the macrofossils for radiocarbon analysis at LARA, the two anonymous reviewers for valuable comments on previous versions of the manuscript and the editor Prof. Vivienne Jones.

Funding

The author(s) disclosed receipt of the following financial support for the research, authorship, and/or publication of this article: This study was funded by the Swiss National Science Foundation (SNF; SNF 200020_182084, SNF 200021_149203 and PMPDP2-122945).

ORCID iDs

Fabian Rey https://orcid.org/0000-0002-0737-3921
Colin J. Courtney Mustaphi https://orcid.org/0000-0002-4439-2590
Sönke Szidat https://orcid.org/0000-0002-1824-6207
Oliver Heiri https://orcid.org/0000-0002-3957-5835

Supplemental material

Supplemental material for this article is available online.

References

Ammann B and Lotter AF (1989) Late-glacial radiocarbon- and palynostratigraphy on the Swiss Plateau. *Boreas* 18: 109–126.

Björck S and Wohlfahrt B (2001) ^{14}C chronostratigraphic techniques in paleolimnology. In: Last WM and Smol JP (eds) *Tracking Environmental Change Using Lake Sediments: Basin Analysis, Coring, and Chronological Techniques*. Dordrecht: Kluwer, pp.204–245.

Blaauw M (2010) Methods and code for 'classical' age-modelling of radiocarbon sequences. *Quaternary Geochronology* 5: 512–528.

Blaauw M and Christen JA (2011) Flexible paleoclimate age-depth models using an autoregressive gamma process. *Bayesian Analysis* 6: 457–474.

Blaauw M, Christen JA, Bennett KD et al. (2018) Double the dates and go for Bayes — Impacts of model choice, dating density and quality on chronologies. *Quaternary Science Reviews* 188: 58–66.

Blaauw M and Heegaard E (2012) Estimation of age-depth relationships. In: Birks HJB, Juggins S, Lotter A et al. (eds) *Tracking Environmental Change Using Lake Sediments, Developments in Paleoenvironmental Research*. Dordrecht: Springer, pp.379–413.

Bolland A, Rey F, Gobet E et al. (2020) Summer temperature development 18000–14000 cal. BP recorded by a new chironomid record from Burgäschisee. Swiss Plateau. *Quaternary Science Reviews* 243: 106484.

Bronk Ramsey C (1994) Analysis of chronological information and radiocarbon calibration: The program OxCal. *Archaeological Computing Newsletter* 41: 11–26.

Bronk Ramsey C (1995) Radiocarbon calibration and analysis of stratigraphy: The OxCal program. *Radiocarbon* 37: 425–430.

Bronk Ramsey C (2001) Development of the radiocarbon calibration program. *Radiocarbon* 43: 355–363.

Bronk Ramsey C (2008) Deposition models for chronological records. *Quaternary Science Reviews* 27: 42–60.

Bronk Ramsey C and Lee S (2013) Recent and planned developments of the program OxCal. *Radiocarbon* 55: 720–730.

Bronk Ramsey C, van der Plicht J and Weninger B (2001) 'Wiggle matching' radiocarbon dates. *Radiocarbon* 43: 381–409.

Brugger SO, Gobet E, van Leeuwen JFN et al. (2016) Long-term man–environment interactions in the Bolivian Amazon: 8000 years of vegetation dynamics. *Quaternary Science Reviews* 132: 114–128.

Dietre B, Walser C, Kofler W et al. (2017) Neolithic to Bronze Age (4850–3450 cal. BP) fire management of the Alpine Lower Engadine landscape (Switzerland) to establish pastures and cereal fields. *The Holocene* 27: 181–196.

Duprat-Oualid F, Rius D, Bégeot C et al. (2017) Vegetation response to abrupt climate changes in western Europe from 45 to 14.7k cal a BP: The Bergsee lacustrine record (Black Forest, Germany). *Journal of Quaternary Science* 32: 1008–1021.

Feeser I, Dörfler W, Czymzik M et al. (2016) A mid-Holocene annually laminated sediment sequence from Lake Woserin: The role of climate and environmental change for cultural development during the Neolithic in northern Germany. *The Holocene* 26: 947–963.

Finsinger W, Schwörer C, Heiri O et al. (2019) Fire on ice and frozen trees? Inappropriate radiocarbon dating leads to unrealistic reconstructions. *New Phytologist* 222: 657–662.

Garcés-Pastor S, Coissac E, Lavergne S et al. (2022) High resolution ancient sedimentary DNA shows that alpine plant diversity is associated with human land use and climate change. *Nature Communications* 13: 1–16.

Gassner S, Gobet E, Schwörer C et al. (2020) 20,000 years of interactions between climate, vegetation and land use in Northern Greece. *Vegetation History and Archaeobotany* 29: 75–90.

Gavin DG (2001) Estimation of inbuilt age in radiocarbon ages of soil charcoal for fire history studies. *Radiocarbon* 43: 27–44.

Gobet E, Tinner W, Hochuli PA et al. (2003) Middle to Late Holocene vegetation history of the Upper engadine (Swiss Alps): The role of man and fire. *Vegetation History and Archaeobotany* 12: 143–163.

Goslar T, van der Knaap WO, Hicks S et al. (2005) ^{14}C dating of modern peat profiles: pre- and post- bomb ^{14}C variations in the construction of age-depth models. *Radiocarbon* 47: 115–134.

Haas M, Kaltenrieder P, Ladd SN et al. (2020) Land-use evolution in the catchment of Lake Murten, Switzerland. *Quaternary Science Reviews* 230: 106154.

Hajdas I, Zolitschka B, Ivy-Ochs SD et al. (1995) AMS radiocarbon dating of annually laminated sediments from Lake Holzmaar, Germany. *Quaternary Science Reviews* 14: 137–143.

Heegaard E, Birks HJ and Telford RJ (2005) Relationships between calibrated ages and depth in stratigraphical sequences: An estimation procedure by mixed-effect regression. *The Holocene* 15: 612–618.

Heiri O, Lotter AF, Hausmann S et al. (2003) A chironomid-based Holocene summer air temperature reconstruction from the Swiss Alps. *The Holocene* 13: 477–484.

Ilyashuk B, Gobet E, Heiri O et al. (2009) Lateglacial environmental and climatic changes at the Maloja pass, Central Swiss alps, as recorded by chironomids and pollen. *Quaternary Science Reviews* 28: 1340–1353.

Kleinmann A, Merkt J and Müller H (2015) Sedimente des degersees: Ein Umweltarchiv – Sedimentologie und Palynologie. In: Mainberger M, Merkt J and Kleinmann A (eds) *Pfahlbausiedlungen Am Degersee, Archäologische und Naturwissenschaftliche Untersuchungen*. Darmstadt: Theiss, pp.409–471.

Kołaczek P, Buczek K, Margielewski W et al. (2021) Development and degradation of a submontane forest in the Beskid Wyspowy Mountains (Polish Western Carpathians) during the Holocene. *The Holocene* 31: 1716–1732.

Lacourse T and Gajewski K (2020) Current practices in building and reporting age-depth models. *Quaternary Research* 96: 28–38.

Lotter AF (1999) Late-glacial and Holocene vegetation history and dynamics as shown by pollen and plant macrofossil analyses in annually laminated sediments from Soppensee, central Switzerland. *Vegetation History and Archaeobotany* 8: 165–184.

Makri S, Rey F, Gobet E et al. (2020) Early human impact in a 15,000-year high-resolution hyperspectral imaging record of paleoproduction and anoxia from a varved lake in Switzerland. *Quaternary Science Reviews* 239: 106335.

Makri S, Wienhues G, Bigalke M et al. (2021) Variations of sedimentary Fe and Mn fractions under changing lake mixing regimes, oxygenation and land surface processes during Lateglacial and Holocene times. *The Science of the Total Environment* 755: 143418.

Martin-Puertas C, Walsh AA, Blockley SPE et al. (2021) The first Holocene varve chronology for the UK: Based on the integration of varve counting, radiocarbon dating and tephrostratigraphy from Diss Mere (UK). *Quaternary Geochronology* 61: 101134.

Marty J and Myrbo A (2014) Radiocarbon dating suitability of aquatic plant macrofossils. *Journal of Paleolimnology* 52: 435–443.

Mellström A, Muscheler R, Snowball I et al. (2013) Radiocarbon wiggle-match dating of bulk Sediments—How accurate can it be? *Radiocarbon* 55: 1173–1186.

Oswald WW, Anderson PM, Brown TA et al. (2005) Effects of sample mass and macrofossil type on radiocarbon dating of arctic and boreal lake sediments. *The Holocene* 15: 758–767.

Pedrotta T, Gobet E, Schwörer C et al. (2021) 8,000 years of climate, vegetation, fire and land-use dynamics in the thermo-Mediterranean vegetation belt of northern Sardinia (Italy). *Vegetation History and Archaeobotany* 30: 789–813.

Reimer PJ, Austin WEN, Bard E et al. (2020) The IntCal20 northern hemisphere radiocarbon age calibration curve (0–55 cal kBP). *Radiocarbon* 62: 725–757.

Rey F, Gobet E, Schwörer C et al. (2019a) Causes and mechanisms of synchronous succession trajectories in primeval Central European mixed *Fagus sylvatica* forests. *Journal of Ecology* 107: 1392–1408.

Rey F, Gobet E, Szidat S et al. (2019b) Radiocarbon wiggle matching on laminated sediments delivers high-precision chronologies. *Radiocarbon* 61: 265–285.

Rey F, Brugger SO, Gobet E et al. (2022) 14,500 years of vegetation and land use history in the upper continental montane zone at lac de Champex (Valais, Switzerland). *Vegetation History and Archaeobotany* 31: 377–393.

Rey F, Gobet E, Schwörer C et al. (2020) Climate impacts on vegetation and fire dynamics since the last deglaciation at Moossee (Switzerland). *Climate of the Past* 16: 1347–1367.

Rey F, Gobet E, van Leeuwen JFN et al. (2017) Vegetational and agricultural dynamics at burgäschisee (Swiss Plateau) recorded for 18,700 years by multi-proxy evidence from partly varved sediments. *Vegetation History and Archaeobotany* 26: 571–586.

Rey F, Schwörer C, Gobet E et al. (2013) Climatic and human impacts on mountain vegetation at Lauenensee (Bernese alps, Switzerland) during the last 14,000 years. *The Holocene* 23: 1415–1427.

Rösch M, Kleinmann A, Lechterbeck J et al. (2014) Botanical off-site and on-site data as indicators of different land use systems: A discussion with examples from southwest Germany. *Vegetation History and Archaeobotany* 23: 121–133.

Rösch M, Stojakowits P and Friedmann A (2021) Does site elevation determine the start and intensity of human impact? Pollen evidence from southern Germany. *Vegetation History and Archaeobotany* 30: 255–268.

Schwörer C, Colombaroli D, Kaltenrieder P et al. (2015) Early human impact (5000-3000 BC) affects mountain forest dynamics in the alps. *Journal of Ecology* 103: 281–295.

Schwörer C, Kaltenrieder P, Glur L et al. (2014) Holocene climate, fire and vegetation dynamics at the treeline in the Northwestern Swiss Alps. *Vegetation History and Archaeobotany* 23: 479–496.

Stuiver M and Polach HA (1977) Discussion: Reporting of ^{14}C data. *Radiocarbon* 19: 355–363.

Stuiver M and Reimer PJ (1993) Extended ^{14}C data base and revised CALIB 3.0 ^{14}C age calibration program. *Radiocarbon* 35: 215–230.

Szidat S, Salazar GA, Vogel E et al. (2014) ^{14}C analysis and sample preparation at the new Bern Laboratory for the analysis of radiocarbon with AMS (LARA). *Radiocarbon* 56: 561–566.

Tinner W, Conedera M, Ammann B et al. (2005) Fire ecology north and south of the Alps since the last ice age. *The Holocene* 15: 1214–1226.

Tinner W, Lotter AF, Ammann B et al. (2003) Climatic change and contemporaneous land-use phases north and south of the Alps 2300 BC to 800 AD. *Quaternary Science Reviews* 22: 1447–1460.

Tinner W and Theurillat J-P (2003) Uppermost limit, extent, and fluctuations of the timberline and treeline ecocline in the Swiss Central Alps during the past 11,500 years. *Arctic, Antarctic, and Alpine Research* 35: 158–169.

Trachsel M and Telford RJ (2017) All age–depth models are wrong, but are getting better. *The Holocene* 27: 860–869.

Vescovi E, Ravazzi C, Arpenti E et al. (2007) Interactions between climate and vegetation during the Lateglacial period as recorded by lake and mire sediment archives in Northern Italy and Southern Switzerland. *Quaternary Science Reviews* 26: 1650–1669.

Zander PD, Szidat S, Kaufman DS et al. (2020) Miniature radiocarbon measurements ($<150\,\mu g\,c$) from sediments of lake żabińskie, poland: effect precision and dating density on age–depth models. *Geochronology* 2: 63–79.

Zander PD, Żarczyński M, Vogel H et al. (2021) A high-resolution record of Holocene primary productivity and water-column mixing from the varved sediments of Lake żabińskie, Poland. *The Science of the Total Environment* 755: 143713.

Zolitschka B, Francus P, Ojala AEK et al. (2015) Varves in lake sediments – A review. *Quaternary Science Reviews* 117: 1–41.